Multi-photon ionization and fragmentation of uracil: neutral excited-state ring opening and hydration effects

Multi-photon ionization and fragmentation of uracil: Neutral excited-state ring opening and hydration effects

B. Barc, M. Ryszka, J. Spurrell, M. Dampc, P. Limão-Vieira, R. Parajuli, N. J. Mason, and S. Eden

Citation: The Journal of Chemical Physics **139**, 244311 (2013); doi: 10.1063/1.4851476
View online: http://dx.doi.org/10.1063/1.4851476
View Table of Contents: http://scitation.aip.org/content/aip/journal/jcp/139/24?ver=pdfcov
Published by the AIP Publishing

Multi-photon ionization and fragmentation of uracil: Neutral excited-state ring opening and hydration effects

B. Barc, M. Ryszka, J. Spurrell, M. Dampc, P. Limão-Vieira,[a] R. Parajuli,[b] N. J. Mason, and S. Eden[c]

Department of Physical Sciences, The Open University, Walton Hall, Milton Keynes MK7 6AA, United Kingdom

(Received 4 November 2013; accepted 4 December 2013; published online 31 December 2013)

Multi-photon ionization (MPI) of the RNA base uracil has been studied in the wavelength range 220–270 nm, coinciding with excitation to the $S_2(\pi\pi^*)$ state. A fragment ion at m/z = 84 was produced by 2-photon absorption at wavelengths ≤232 nm and assigned to $C_3H_4N_2O^+$ following CO abstraction. This ion has not been observed in alternative dissociative ionization processes (notably electron impact) and its threshold is close to recent calculations of the minimum activation energy for a ring opening conical intersection to a $\sigma(\text{n-}\pi)\pi^*$ closed shell state. Moreover, the predicted ring opening transition leaves a CO group at one end of the isomer, apparently vulnerable to abstraction. An MPI mass spectrum of uracil-water clusters is presented for the first time and compared with an equivalent dry measurement. Hydration enhances certain fragment ion pathways (particularly $C_3H_3NO^+$) but represses $C_3H_4N_2O^+$ production. This indicates that hydrogen bonding to water stabilizes uracil with respect to neutral excited-state ring opening. © *2013 AIP Publishing LLC*. [http://dx.doi.org/10.1063/1.4851476]

I. INTRODUCTION

The electronic excitation and ionization dynamics of nucleobases have attracted interest for many years with the central aim of understanding the pathways that can initiate reactivity and the formation of DNA and RNA lesions.[1] Isolated molecules are the natural starting point to probe the photophysics, while parallel studies on pure and mixed clusters enable closer analogies to be drawn with biological environments where different isomeric forms, intermolecular energy transfer processes and reactivity can be significant.

The present experiments probe the pyrimidine derivative base uracil ($C_4H_4N_2O_2$), which forms two hydrogen bonds with adenine in RNA. Its close structural similarity with the DNA base thymine adds to the interest in this molecule, particularly with respect to differences in the photophysical properties of the two bases and their possible radiobiological consequences.[2] A series of ultrafast spectroscopy and computational chemistry studies (e.g., Refs. 3–5) have significantly advanced our understanding of the radiationless decay pathways from the bright $\pi\pi^*$ state of uracil in isolation as well as within certain hydrated complexes and base-pairs. In particular, theoretical calculations have identified ring opening[6] and tautomeric transitions[2] in electronic excited states. This provides the impetus for our experiments as well as the essential context for the proposed interpretations. Due to the possibility of neutral excited state transitions in the stepwise excitation process, MPI can activate channels that are closed in single-photon absorption or collision induced ionization experiments where ionic states are directly accessed from the electronic ground state.[7] Accordingly, the first aim of the present work was to study fragment ion production by MPI as a tool to observe evidence for excited state transitions. These were recognizable via major differences between MPI and electron impact ionization (EII) mass spectra and distinct wavelength thresholds for the production of specific fragment ions. Although time resolved analysis was not possible, the present MPI scheme using single-color nanosecond-timescale laser pulses enabled the initial excitation to be carried out in a much wider wavelength range (220–270 nm) than any previous study. Furthermore, we performed the first experimental comparison of uracil MPI in dry and hydrated clustering conditions in order to advance our understanding of how the local water environment can modify the molecule's response to UV excitation and ionization. This question has attracted considerable interest with respect to the specific excitation and relaxation dynamics[8–10] but no previous research has directly addressed hydration effects on the fragmentation pathways of the excited molecule or ion.

II. EXPERIMENTAL

The experimental system developed for these studies is described here for the first time. As shown in Fig. 1, argon seeded with vaporized uracil and/or water flowed through a CW nozzle into a pumped chamber to form a supersonic jet. The jet passed through a skimmer and crossed a pulsed UV laser beam for MPI measurements or an electron beam from a commercial gun (*Kimball ELG*-2) for EII experiments. The resulting ions were detected using a *reflectron* time-of-flight (TOF) mass spectrometer.

[a]Permanent address: Laboratório de Colisões Atómicas e Moleculares, CEFITEC, Departamento de Física, Faculdade de Ciências e Tecnologia, Universidade Nova de Lisboa, 2829-516 Caparica, Portugal.
[b]Permanent address: Department of Physics, Amrit Campus, Tribhuvan University, Kathmandu, Nepal.
[c]Author to whom correspondence should be addressed. Electronic mail: s.p.eden@open.ac.uk

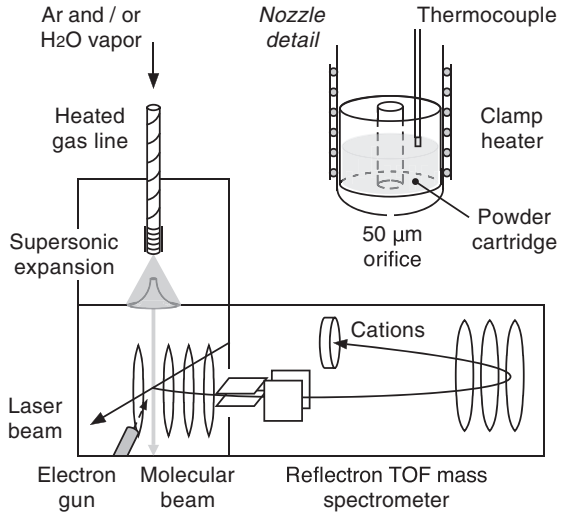

FIG. 1. Schematic view of the experimental system.

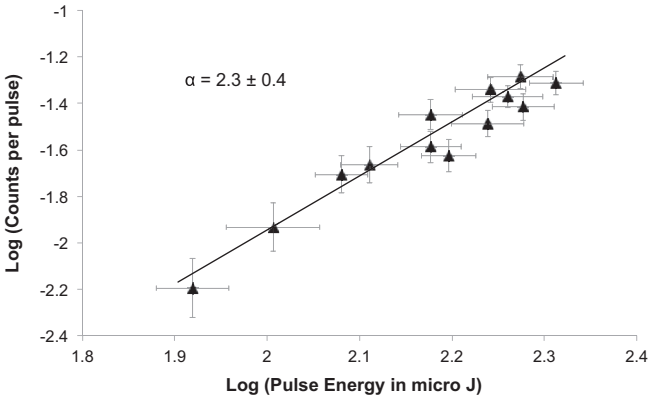

FIG. 2. Power dependence (α = photon order) of uracil MPI on laser pulse energy. The measurement was carried out at 220 nm with average fluence (3–7) × 10^5 W cm^{-2}.

The expansion chamber, interaction chamber, and mass spectrometer flight tube were evacuated using 520, 600, and 150 l s^{-1} turbo pumps, respectively. The 50 μm diameter nozzle was laser-drilled into the closed end of a stainless steel tube (*Lennox Laser*). The outside of the tube was heated using a coiled resistive heater with an axial clamp in order to sublimate the uracil (Sigma-Aldrich, minimum purity 99%) in a stainless steel powder cartridge positioned above the nozzle. A thermocouple was inserted directly into the powder and the uracil temperature was held at 250 °C. This is comparable with or lower than vaporization temperatures adopted in previous studies that reported no evidence for thermally driven decomposition, isomerization, or reactivity.[11] The experiments targeting isolated uracil molecules were recorded with an argon pressure of 0.6 bar. This is lower than the driving pressures applied in previous supersonic expansion experiments probing isolated uracil[12] and accordingly no evidence was observed for uracil cluster ions or their derivative UH^+ (see Sec. III B) in the measurements presented in Figures 2–5 and Tables I and II. The skimmer (*Beam Dynamics model* 2, orifice diameter 400 μm) was heated to 125 °C to prevent condensation. A stainless steel H_2O reservoir was connected

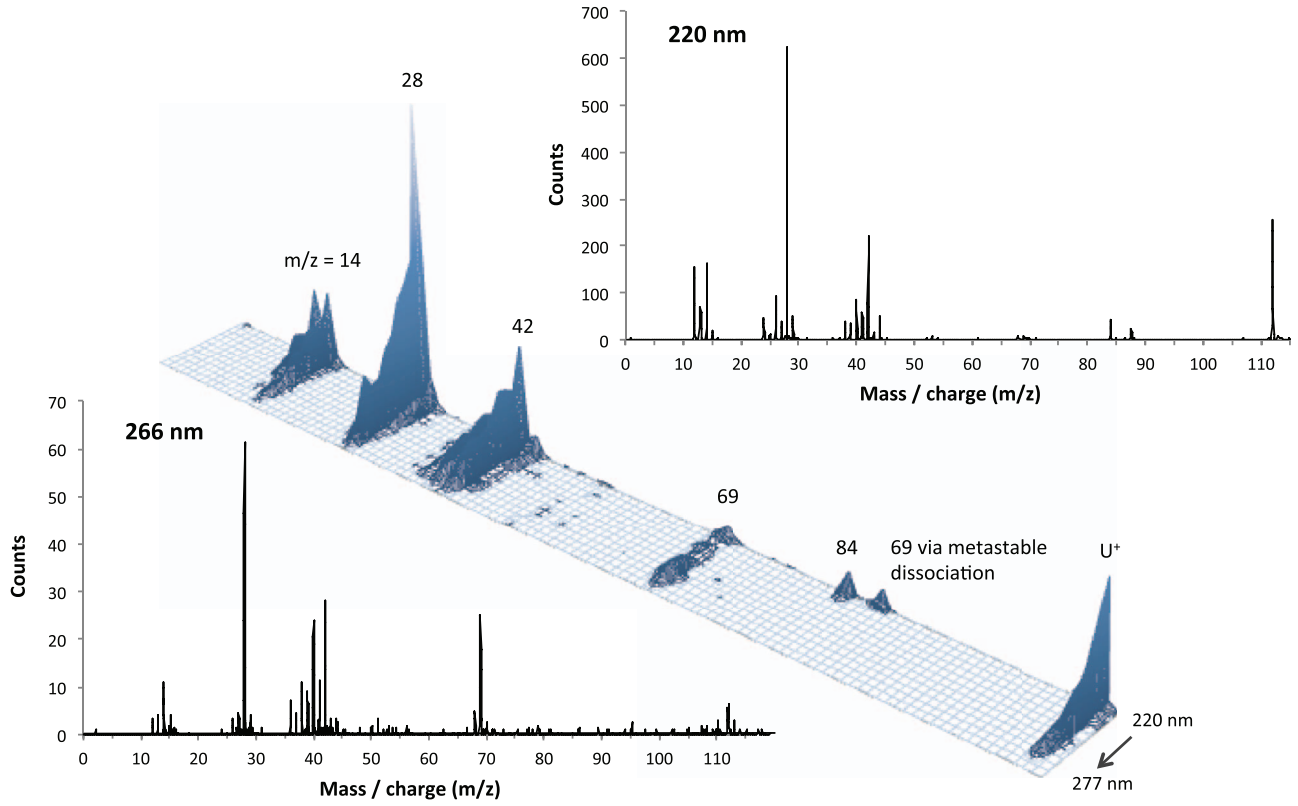

FIG. 3. Wavelength dependence of uracil MPI. Mass spectra with 10^4 laser pulses were recorded at 2–7 nm intervals in the range 220–277 nm with average fluence 7×10^7 W cm^{-2}.

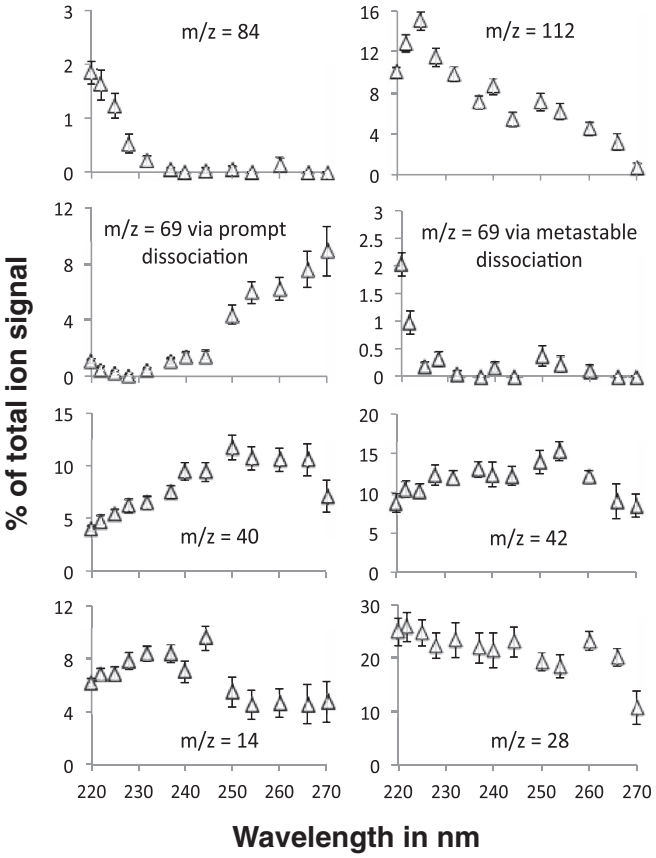

FIG. 4. MPI wavelength (220–270 nm) dependence of selected ion counts/total counts. Fluence and molecular beam conditions match Fig. 3.

to the buffer gas line via a valve. The reservoir and the gas line were heated using resistive wire and the H_2O temperature was monitored using a thermocouple in contact with the reservoir wall. The resistive wire was wrapped more sparsely around the reservoir than around the gas line in order to prevent condensation.

The third harmonic output (355 nm) of an Nd:YAG laser system (*Continuum Powerlight II 8000*) provided the pump source for a dye laser (*Sirah Cobra-Stretch*). Coumarin dyes gave access to the wavelength range 220–277 nm and a diffraction grating with groove density 1800 lines/mm enabled the wavelength to be selected with a resolution better than 10^{-3} nm. The pulse width and frequency were 7 ns and 10 Hz. The average laser pulse energy was adjusted in the range 100–2000 μJ by changing the delay between the pulses triggering the xenon flash lamps and the *Q-switch* of the Nd:YAG laser. A convex lens on a slider was used to control the laser spot diameter (3 mm without the lens) at the interaction with the molecular beam. Whereas average fluence values could be determined, we did not have a measure of the temporal fluence structure during pulses (discussed further in Sec. III A).

The reflectron mass spectrometer was designed and constructed by KORE technology, while its voltage divider system was home-built. Following extraction in a -320 V cm^{-1} field, acceleration to -2 kV, and deflection to compensate for the molecular beam velocity, the cations passed through the field-free part of the flight tube and the reflectron optics. The voltage on the final reflectron electrode could be adjusted to test for metastable dissociation; a fragment ion formed some time after ionization will have lower KE than an equivalent fragment ion produced by prompt dissociative ionization and can therefore be reflected by a lower potential difference. The discrete dynode electron multiplier detector included a -10 kV post-acceleration grid to increase the detection efficiency of high-mass ions. The pre-amplified ion signals were timed using a 250 ps resolution *Fast Comtec P7887* time-to-digital conversion (TDC) card. The highest mass resolution we have attained to date was m/Δm = 2000 using a focused laser beam. A data acquisition system was developed to record the laser pulse energy and the number of ions detected within a given flight time range on a pulse-by-pulse basis. The system was based on a *LabView* application interfacing

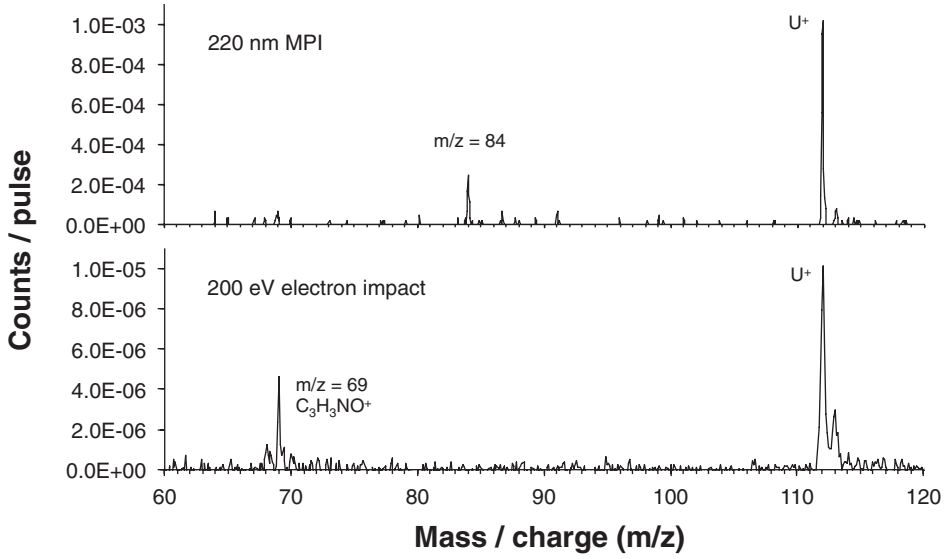

FIG. 5. Comparison of MPI (220 nm, average fluence 6×10^7 W cm^{-2}) and electron impact ionization (200 eV) mass spectra recorded with matching molecular beam conditions.

TABLE I. Product ions observed following the ionization of gas-phase uracil ($C_4H_4N_2O_2$) by 20 eV photons,[21] by fast electrons,[23,24] and by MPI at 220 nm (Fig. 3 inset).[a]

Mass/ charge (m/z) (where available, intensity is given as a percentage of the strongest peak)				
	70 eV e^- impact			
220 nm MPI (present work)	Imhoff *et al.*[23]	Rice *et al.*[24]	20 eV photo-ionization[21]	Proposed ion formula
113 (2%)	113	…	…	$C_4H_4N_2O_2^+$ with one ^{13}C
112 (39%)	112	112 (78%)	112 (63%)	$C_4H_4N_2O_2^+$
…	…	96 – weak	96 – weak	…
84 (8%)	…	…	…	$C_3H_4N_2O^+$
…	…	77 – weak	…	…
…	70[b]	70 (7%)	70 - weak	$C_3H_4NO^+$[21,37]
69 *meta* (6%)[c]	…	…	…	Uracil$^+$* dissociation after 1.3–14.6 μs producing $C_3H_3NO^+$
69 (4%)	69	69 (63%)	69 (52%)	$C_3H_3NO^+$[5,21,37]
68 (2%)	68	68 (33%)	68 (33%)	$C_3H_2NO^+$[21]
…	67	67 - weak	…	…
…	56	56 - weak	56 - weak	…
…	53	53 - weak	53 - weak	…
…	52	52 - weak	52 - weak	…
…	51	51 - weak	…	…
44 (5%)	44	44 (8%)	44 -weak	CH_2NO^+[23]
43 (4%)	43	43 (15%)	43 (10%)	$CHNO^+$[21]
42 (34%)	42	42 (100%)	42 (100%)	$C_2H_2O^+$[5,21,37]/$C_2H_4N^+$[23,37]
41 (10%)	41	41 (48%)	41 (50%)	$C_2H_3N^+$[5,21]/C_2HO^+[21]]
40 (17%)	44	40 (57%)	40 (25%)	$C_2H_2N^+$[21]
39 (7%)	39	39 (15%)	39 - weak	C_2HN^+
38 (6%)	38	38 (7%)	…	C_2N^+
…	30	…	…	…
29 (9%)	29	29 - weak	29 - weak	CH_3N^+[21,37]/HCO^+[21]
28 (100%)	28	28 (78%)	28 (86%)	CH_2N^+[5,21,37]/CO^+[3]
27 (7%)	27	27 - weak	27 - weak	CHN^+[21]
26 (18%)	26	26 - weak	26 (5%)	$C_2H_2^+$[21]
25 (3%)	25	…	…	C_2H^+
24 (9%)	24	…	…	C_2^+
…	18	Not measured	18 – weak	H_2O^+ impurity[21]
…	17		17 – weak	NH_3^+[21]
…	16		…	…
15 (2%)	15		…	CH_3^+[23]
14 (24%)	14		14 – weak	N^+[21]/CH_2^+[23]
13 (4%)	13		Not available	CH^+
12 (22%)	12			C^+
…	2			…
1 (1%)	1			H^+[23]

[a]The present data columns only include peaks with count rates that are clearly greater than background measurements. In the columns summarizing the data of Jochims *et al.*[21] and Rice *et al.*,[24] channels with intensities <5% of the maximum peak are labeled weak. Arani *et al.*[37] reported other possible assignments but proposed those cited above as the most probable.

[b]Imhoff *et al.*[23] suggested that $C_3H_3NO^+$ including a ^{13}C isotope might contribute to this peak.

[c]This metastable channel appears at m/z = 87.6 in the calibrated mass spectra shown in Fig. 3.

with the TDC card and the laser pulse energy meter (*Spectrum Detector SPJ-D-8*).

III. RESULTS AND DISCUSSION

A. Non-dissociative MPI of isolated uracil

Uracil molecules were multi-photon ionized in the wavelength range 220–270 nm with average fluence 10^5–10^8 W cm^{-2}. Previous single-color MPI experiments using ns laser pulses at 222 nm,[13] 248 nm,[14] and 235–268 nm[12] did not produce any discernible uracil cation signals, whereas Brady *et al.*[15] were able to record a REMPI spectrum with a 270–285 nm pump and a 193 nm probe (both ns-timescale pulses). Fig. 2 shows weak U^+ production ($\sim 10^{-2}$ counts / pulse) at 220 nm as a function of laser pulse energy. The photon order (α) can be estimated from the ion counts per pulse (I) and the laser pulse energy (E) using the perturbation theory expression $I = cE^{\alpha}$, where c is a constant.[16] Saturation at any absorption stage reduces the power dependence so the measured α provides a minimum for the number of photons absorbed in

TABLE II. Photon orders for the production of selected fragment ions from gas-phase uracil irradiated at 220 nm (5.64 eV). Where available, previous photo-ionization appearance energies (AE) are given.[21]

	Photon order (α) for different product ions (mass/charge in Th)								
Average fluence (W cm^{-2})	112 (AE 9.15 eV)	84	69 *meta*[a]	69 (AE 10.95 eV)	42 (AE 13.25 eV)	40 (AE 14.06 eV)	28 (AE 13.75 eV)	14	12
3×10^5–7×10^5	2.3 ± 0.4[b]	2.0 ± 0.3	2.1 ± 0.8	…[c]	3.0 ± 0.9	…[c]	3.5 ± 0.9	…[c]	…[c]
1×10^6–5×10^6	1.5 ± 0.2	1.1 ± 0.2	1.1 ± 0.2	1.5 ± 0.4	2.1 ± 0.3	1.7 ± 0.2	2.6 ± 0.3	2.9 ± 0.6	…[c]
9×10^6–6×10^7	0.2 ± 0.1	0.3 ± 0.2	0.1 ± 0.2	0.1 ± 0.2	0.7 ± 0.1	0.6 ± 0.1	1.2 ± 0.1	1.4 ± 0.1	2.4 ± 0.2

[a]Uracil^{+}* dissociation after 1.3–14.6 μs producing $C_3H_3NO^+$.
[b]Shown in Fig. 2.
[c]Insufficient counts to derive a photon order.

the ionization process. To reduce possible saturation effects, the data in Fig. 2 were measured at average fluence (3–7) $\times$ 10^5 W cm^{-2}, close to the minimum required to accumulate adequate statistics. The observed photon order of 2.3 ± 0.4 indicates 2-photon ionization.

Earlier time-resolved experiments on gas-phase uracil with relatively high pump wavelengths (250 and 267 nm) did not provide evidence for access to states with ns-order lifetimes.[3,4,17] He *et al.*[10,18] observed access to long-lived (23–209 ns) dark states of thymine, methylated thymine, and methylated uracil, as well as a general tendency for longer lifetimes at lower excitation wavelengths (approx. range 290–220 nm) and higher degree of methyl substitution (up to two sites). They were not able to measure uracil and attributed this to the limitations of their pulsed valve as opposed to the molecule's photo-physical properties. Etinski *et al.*[19] theoretically characterized the lowest lying electronic states of uracil and performed calculations indicating that the $T_1(\pi\pi^*)$ state is populated from the $S_1(n\pi^*)$ state on a sub-nanosecond time scale. However, single photon ionization from this triplet state is unlikely in the present energy range (5.64–4.60 eV) in view of its low vertical excitation energy (3.65 eV from Abouaf *et al.*'s EELS measurements cited as a private communication by Nguyen *et al.*[20]) compared with the ionization energy of uracil (9.15 ± 0.03 eV[21]). Therefore, the most plausible 2-photon pathway in the present experiments involves ionization from the state previously characterized by exponential decay with a time constant of 2.4 ps.[4,17] This state (S_1) is understood to have predominantly $n\pi^*$ character and is accessed by rapid (<50 fs) internal conversion following excitation to the bright $S_2(\pi\pi^*)$ state (see Figure 8 in Nachtigallova *et al.*[6] for a schematic representation). The average fluence values in the Fig. 2 measurement suggest that successive photon absorption on a ps-timescale would be rare. However, higher longitudinal modes can lead to fluence peaks during ns-timescale laser pulses.[22] Indeed, the fact that we observed MPI processes known to occur via virtual excited states (2 + 1 ionization of H and CO discussed in Sec. III C) at an average fluence of 10^8–10^9 W cm^{-2} provides a strong indication that our laser pulses contained fluence peak structure that can also account for photo-excitation from the S_1 state.

B. Fragment ion production in MPI and EII of isolated uracil

Fig. 3 shows uracil MPI mass spectra as a function of wavelength in the range 220–277 nm. The average fluence in these measurements was 7×10^7 W cm^{-2}, leading to significant production of fragment ions. Table I lists the peaks observed at 220 nm. Dissociative ionization of uracil has been studied extensively by electron impact,[23–28] ion impact,[28–35] and single photon absorption.[21] Taking into account differences in energy deposition and signal/noise ratios, the previous experiments were broadly consistent in terms of the fragment ions produced and three high-resolution examples are summarized in Table I. The only previous measurements probing fragment ion production in uracil MPI were carried out using a 260 nm pump (~50 fs) and a 780 nm probe (40 fs) with a variable delay of up to 10 ps.[5,36] These previous MPI mass spectra showed no clear evidence for fragment ions that were not observed in the earlier collision and photoabsorption experiments.

On the basis of appearance energies and thermochemical data, Jochims *et al.*[21] proposed that the dominant fragmentation pathways of the excited uracil radical cation involve HNCO loss followed by $C_3H_3NO^+$ (m/z = 69) dissociation (particularly H, CO, HCN, and HCNH loss). Matsika *et al.*'s[5,36] *ab initio* calculations also supported sequential fragmentation via $C_3H_3NO^+$ as the mechanism to produce the strong fragment ions at m/z = 42, 41, and 28. Only in the case of ion production at m/z = 28 was direct dissociation of the radical cation energetically competitive with the minimum sequential fragmentation pathway. DFT calculations by Arani *et al.*[37] identified plausible sequential fragmentation routes via $C_3H_3NO_2^{\bullet+}$ (85 Th) or $C_3H_4NO^+$ (70 Th), as well as pathways via $C_3H_3NO^{\bullet+}$ (69 Th). Table II shows photon orders for the strongest product ions recorded at 220 nm in three fluence ranges corresponding to different degrees of saturation, as well as previously measured single photon ionization appearance energies.[21] As would generally be expected, the fragment ions with appearance energies >11.28 eV (twice the energy of the 220 nm photons) have photon orders that are greater than uracil$^+$.

Fig. 3 and Table I demonstrate ion production at m/z = 84 by MPI at 220 nm. Fig. 4 shows that the relative production of this fragment ion increased with falling wavelength and that its production threshold was between 237 and 232 nm (5.29 ± 0.06 eV). No previous experiment has produced this fragment ion. We measured a 200 eV EII mass spectrum in molecular beam conditions that matched our MPI experiments (Fig. 5). In agreement with the previous work, strong EII signals were obtained at m/z = 112 and 69 but no peak was observed at 84. The first interpretation we considered

was that the new fragment ion may be traced to ionization of a neutral fragment following dissociative ionization of uracil. A process of this kind would have relatively high photon order. For example, consider Matsika *et al.*'s[5,36] proposed pathway for CH_2N^+ (28 Th) and $C_3H_2NO_2$ (84 atomic mass units) production via direct dissociation of the uracil radical cation. To produce $C_3H_2NO_2^+$ via this process would require at least one more photon than CH_2N^+ production. Table II shows that the error boundaries of $\alpha(84)$ and $\alpha(112)$ overlap in all three fluence conditions probed, while $\alpha(28)$ is ~1 photon greater. Hence the m/z = 84 ions were produced by 2-photon absorption and any hypothetical *dissociative ionization followed by neutral fragment ionization* pathway can be discounted. The production of the new fragment ion must therefore depend on a process that occurs in a neutral excited state. This process is bypassed when uracil is excited directly to an ionic state, as in the present and previous EII measurements. The possible candidates for this neutral excited state process are dissociation (an excited radical fragment can plausibly be ionized by subsequent single photon absorption) or a transition into an isomeric state with its own distinct dissociative ionization pathways. The absence of the m/z = 84 peak in the previous MPI experiments[5] can be attributed to the 260 nm pump photons having insufficient energy to overcome the dissociation or isomeric transition barrier.

Nachtigallova *et al.*[6] carried out non-adiabatic dynamics simulations of the decay mechanisms of uracil following excitation to the bright S_2 state. In particular, they calculated the stationary points and minima on the crossing seams of the S_2 and S_1 excited states and the electronic ground state (S_0) at the CASSCF, MR-CISD, and MS-CASPT2 levels. From our perspective, the most interesting relaxation pathway is $S_2(\pi\pi^*)$–$S_1(\sigma(\text{n-}\pi)\pi^*)$–$S_0$ with ring opening at the S_2/S_1 crossing seam. Indeed, Nachtigallova and co-workers predicted that this ring opening deactivation pathway *leads almost certainly to new photochemical products*. Two aspects of this pathway specifically link it to the ion at m/z = 84. First, the CASSCF minimum energy of 5.25 eV for the S_2/S_1 crossing seam matches the 5.29 ± 0.06 eV threshold for the present m/z = 84 signal. The equivalent MR-CISD, MR-CISD with Pople corrections, and MS-CASPT2 minimum energies (5.97, 5.57, and 5.84 eV, respectively) agree less closely with the present threshold but are nonetheless consistent with an effect that is only observed significantly above the S_2 band origin (Etinski *et al.*'s[19] calculations using four methods placed the adiabatic energy between 3.74 and 4.03 eV). Second, the predicted ring opening transition leaves a CO group at one end of the structure (shown in Nachtigallova *et al.*'s[6] Figure 2). Therefore CO loss following photoionization of this electronically excited isomer appears to be probable, leaving $C_3H_4N_2O^+$ with m/z = 84. Hence the calculations provide a compelling argument to assign the new MPI fragment ion and, equally, the present experimental results support the theoretically predicted ring-opening pathway.

The present MPI measurements revealed a metastable dissociation pathway, apparent in Fig. 3 as a peak centered at m/z = 87.6. By measuring the cut-off reflection voltage to determine the ion's KE and by comparing its flight time at different mass spectrometer voltages with calculated flight times, we were able to assign the peak unambiguously to uracil$^+$ dissociation in the TOF drift tube producing m/z = 69 fragment ions (1.3–14.6 μs after the laser pulse). Interestingly, Fig. 4 shows that this metastable dissociation signal was above the background level at ≤222 nm but not at 224 nm (threshold 5.61 ± 0.03 eV), whereas prompt (<10 ns after ionization) ion production at m/z = 69 increased steadily with wavelength as a percentage of total ionization. Table II indicates that both peaks were produced by 2-photon ionization at 220 nm (5.64 eV), consistent with the 10.95 eV appearance energy for the m/z = 69 fragment in previous photoionization experiments.[21] Further research is necessary to understand the mechanisms underpinning the prompt and metastable production channels of m/z = 69 ions (widely assigned to $C_3H_3NO^+$) from uracil and their contrasting MPI wavelength dependences. Note that metastable dissociation channels could not be distinguished in the present EII data (Fig. 5) because the ions were not produced at precisely defined times; the electron beam was continuous and the TOF start coincided with the pulsed extraction voltage.

Further to the channels discussed above, Fig. 4 shows the wavelength dependence of four smaller fragment ions and uracil$^+$ as a percentage of total ionization. The m/z = 42, 40, 28, and 14 signals (assigned in Table I and shown to be ≥3 photon ionization processes in Table II) did not show threshold behavior in the 220–270 nm range, while the relative production of uracil$^+$ decreased steadily with increasing wavelength (threshold 4.62 ± 0.03 eV). The latter effect can be rationalized if we assume that higher order (≥3) photon absorption almost exclusively causes dissociative ionization. At photon energies only slightly above half the single photon ionization energy (9.15 ± 0.03 eV[21]), 2 photon ionization will be very weak whereas ≥3 photon ionization can occur relatively efficiently as long as the S_2-S_1 pathway is accessible. As discussed above, several previous experiments have clearly shown S_2-S_1 deactivation following excitation at 4.64 eV.[3,4,17]

C. Neutral fragment production

To our knowledge, neutral fragments of uracil following dissociation in neutral or ionic states have not been observed directly in any previous experiments. The high laser fluence (average 10^8–10^9 W cm^{-2}) measurements in Fig. 6 show an enhancement of the H$^+$ signal from uracil at the 243.1 nm (2 + 1) resonant wavelength for hydrogen MPI.[38] Jochims *et al.*[21] assigned the m/z = 68 fragment ion to H loss from $C_3H_3NO^+$ on the basis of appearance energies and thermochemical calculations, although this is clearly not the only plausible pathway for neutral H production. We have a particular interest in CO as this is the neutral by-product of the mechanism that we associate with ion production at m/z = 84 (see Sec. III B). Fig. 6 demonstrates strong enhancement of the m/z = 28 signal at the 230.05 nm resonance for CO MPI.[39,40] While this is broadly consistent with the proposed m/z = 84 pathway, Jochims *et al.*[21] proposed competitive neutral CO loss mechanisms within the sequential fragmentation processes producing the prominent ions at m/z = 41 ($H_3C_2N^+$) and 40 ($C_2H_2N^+$) (see Table I).

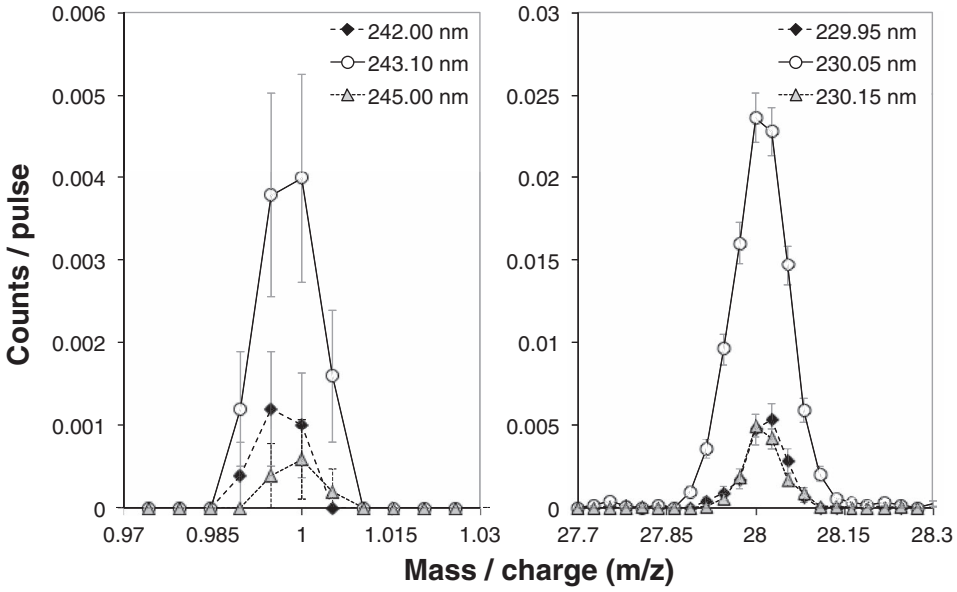

FIG. 6. Uracil mass spectra showing enhanced MPI at 2 + 1 resonant wavelengths for hydrogen (243.10 nm, left) and CO (230.05 nm, right). The measurements were carried out at the maximum laser fluence (average 10^8–10^9 W cm^{-2}) for the present system.

D. Hydrated clusters

Whereas various theoretical studies have been carried out on uracil-water clusters,[41–46] experimental studies are scarce. The present work provides the first MPI mass spectrum of uracil-water clusters. To our knowledge, the only MPI measurement of uracil clusters in the literature was recorded in dry conditions by Kim *et al.*[47] using 274 nm ns-timescale laser pulses. The same group reported EII mass spectra of hydrated uracil clusters showing evidence for $U_mH^+(H_2O)_n$ series as well as $U_m{}^+(H_2O)_n$.[48] The only previous experiment in the literature that explored clustering effects on fragment ion production from uracil (dry clusters only) was carried out for 100 keV O^{5+} impact ionization.[32] Signals at m/z = 83 (U^+ minus HCO) and 95 (U^+ minus OH) were only observed in clustering conditions and were linked to hydrogen bonding effects, as opposed to stacking. Mass spectra showing the differences between dry and hydrated MPI are presented in Fig. 7. A summary of the observed ion intensities is presented in Table III. No evidence for new fragment ion channels from uracil due to clustering was observed in the present data.

He *et al.*[10] reported that hydration significantly represses access to the long-lived triplet states of methyl-substituted uracil and thymine. In this context, the fact that the total MPI count rate is only reduced by 22% ± 3% due to clustering with water (Fig. 7 and Table III) provides an indicator that the dominant excitation pathways in the present experiments do not involve these triplet states. Further arguments for assigning our MPI signals to photo-excitation in the S_1 state

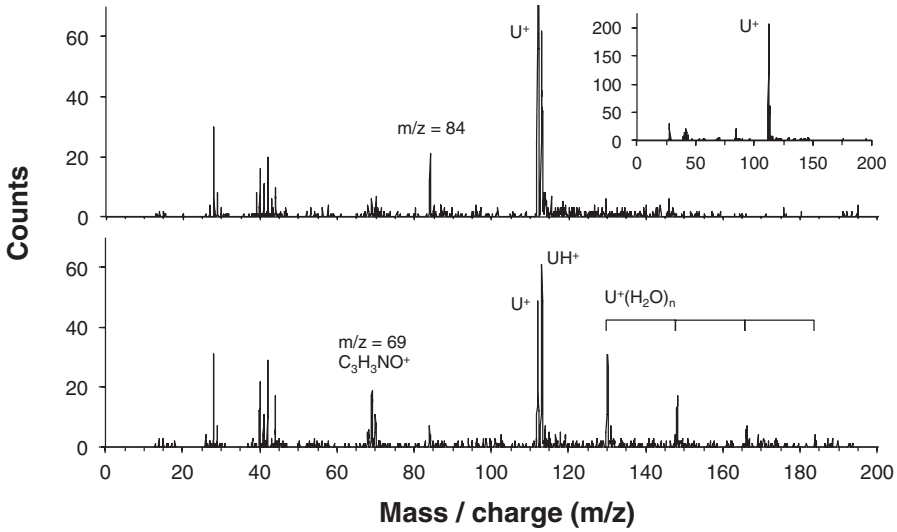

FIG. 7. Single-color MPI (220 nm, average fluence 4 × 10^6 W cm^{-2}, Ar 0.8 bar) of uracil in dry (upper plot and inset) and hydrated conditions (lower plot, water 60 °C).

TABLE III. Hydration effects on the production of ions, cluster ions, and selected fragment ions following uracil MPI at 220 nm. The corresponding mass spectra are shown in Fig. 7. The total ion counts in 10^4 laser pulses were 1960 (including 640 fragment ions) and 1520 (including 670 fragment ions) in dry and hydrated conditions, respectively.

Selected ion		% of total ion counts	
Mass/charge (m/z)	Assignment	Dry	Hydrated
225	U_2H^+ and U_2^+ isotopes	0.3 ± 0.2	...
224	U_2^+	0.2 ± 0.1	0.6 ± 0.3
184	$U^+(H_2O)_4$	...	0.7 ± 0.3
166	$U^+(H_2O)_3$	...	1.6 ± 0.5
148	$U^+(H_2O)_2$	...	5 ± 1
130	$U^+(H_2O)$	...	13 ± 2
113	UH^+ and U^+ isotopes	17 ± 2	21 ± 2
112	U^+	50 ± 3	15 ± 2
<112	All fragment ions[a]	33 ± 2	44 ± 3
84	$C_3H_4N_2O^+$	4 ± 1	1.8 ± 0.5
69 *meta*[b]	U^{+}* dissociation after 1.3–14.6 μs producing $C_3H_3NO^+$	1.8 ± 0.5	0.7 ± 0.3
69	$C_3H_3NO^+$	1.1 ± 0.3	7 ± 1
42	$C_2H_2O^+$ / $C_2H_4N^+$	4 ± 1	3 ± 1
40	$C_2H_2N^+$	4 ± 1	1.2 ± 0.4
28	CH_2N^+ / CO^+	6 ± 1	7 ± 1

[a]Includes counts for fragment ions that have not been included in the table.
[b]This metastable channel appears at m/z = 87.6 in the calibrated mass spectra shown in Fig. 3 and Fig. 7.

(predominantly $n\pi^*$ character with ps-order lifetime) are discussed in Secs. III A and III B.

Table III and Fig. 7 show that the signal at m/z = 69 ($C_3H_3NO^+$, recognized as the precursor to further strong dissociation channels) was markedly stronger in the hydrated measurement. This result may be attributed to energy removal from the excited uracil cation via cluster dissociation tending to stop certain sequential fragmentation processes at an early stage. The reduction in the signal at m/z = 40 (assigned to H loss from $C_3H_3NO^+$, followed by CO loss) due to hydration is consistent with this interpretation. By contrast, other ion signals linked to $C_3H_3NO^+$ fragmentation (e.g., m/z = 28) did not change significantly. Therefore the presently observed hydration effects on the dissociative MPI pathways of uracil cannot be understood purely on the basis of generalized energetic arguments. This is unsurprising as theoretical studies have demonstrated shifts (generally stabilization) of the $^1\pi\pi^*$ and $^1n\pi^*$ states of uracil and their relaxation dynamics[8,9] due to hydrogen bonding with water, as well increased excited-state tautomerization.[2] In this context, it is interesting that the production of the m/z = 84 fragment ion was repressed by hydration in the present data. The result may indicate that the presence of hydrogen-bonded water moieties decouples the excited states involved in the ring-opening conical intersection associated with this dissociative MPI channel (see Sec. III B). Further work is necessary to establish the specific mechanism but it is clear that clustering with water stabilizes uracil with respect to this type of UV-induced damage.

Significant production of ions with m/z = 113 was observed both in the dry and hydrated measurements: ~34% and ~140% of the respective signals at m/z = 112. These peaks are assigned to protonated uracil (UH^+) and a small contribution due to carbon isotopes in uracil (5.2%[49]). UH^+ has been detected following electron collisions with $U_m(H_2O)_n$[48] but the previous papers on the ionization of dry uracil clusters[32,47] did not mention this product. Its production evidently involves intermolecular hydrogen or proton transfer and its presence in the dry mass spectrum shows that the process does not require the presence of water. Indeed, water is transparent at 220 nm[50] so UH^+ production in the present experiments must begin with uracil excitation. Zadorozhnaya and Krylov's[51] calculations showed that the hydrogen-bonded uracil dimer cation relaxes to a proton-transferred form that is much more strongly bound than the most stable stacked or T-shaped dimer cation configurations. Therefore, we attribute the present UH^+ MPI signals to a negative barrier reaction from U^+U to UH^+(U–H) followed by cluster ion dissociation. This interpretation is broadly consistent with the absence of $UH^+(H_2O)_n$ peaks in the MPI mass spectrum (conversely, these species were observed by electron impact ionization[48] and attributed to water ionization followed by proton transfer to uracil). Due to the weaker binding energies of uracil and water molecules,[52] UH^+(U–H) fissure can be expected to involve extensive water loss.

While clustering with water is evidently not essential in the presently observed MPI-induced proton transfer processes, it is interesting to note that the hydrated measurement in Fig. 7 shows a strong increase in the UH^+ signal. This may indicate that the presence of water in the expansion aids the formation of complexes with two or more uracil molecules. It should also be noted that MPI-induced proton transfer might play a role in determining the observed clustering effects on fragment ion production discussed above.

IV. CONCLUSIONS

Previous studies have identified mechanisms by which hydration tends to increase the photo-stability of uracil, notably shifting key singlet states to higher energies[8,9] and restricting intersystem crossing into long-lived triplet states.[10] The present work provides the first experimental evidence for another UV damage process in uracil – theoretically predicted excited state ring opening[6] indicated by the MPI wavelength dependence of a new fragment ion at m/z = 84 – and demonstrates that this is also stabilized by clustering with water. Further research is necessary to understand the specific mechanism responsible for this hydration effect. Additional new results include the observation of a metastable dissociation channel of the uracil radical cation producing $C_3H_3NO^+$, neutral CO fragments, and UH^+ production attributed to proton transfer between hydrogen-bonded uracil dimer ions. The present MPI data enhance our understanding of the unimolecular and intermolecular reactive processes induced by the electronic excitation and ionization of uracil in isolation and in hydrogen-bonded complexes that represent simple models for biological environments.

ACKNOWLEDGMENTS

The authors are grateful for the expert technical support provided by F. Roberston, R. Bence, M. Percy, and C. Hall at the Open University (OU). The contributions of P. Cahillane, K. Pisklova, Z. El-Otell, E. Al Jabbour Maalouf, P. Thorn, and J. Tabet to the experimental development are acknowledged. S.E. acknowledges the support of the British EPSRC through a Life Sciences Interface Fellowship (EP/E039618/1), a Career Acceleration Fellowship (EP/J002577/1), and a Research Grant (EP/L002191/1). S.E. and P.L.-V. acknowledge the support from the British Council for the collaboration between the OU and the Universidade Nova de Lisboa. P.L.-V. acknowledges his visiting Professor position at the OU and support from the Portuguese research grants PEst-OE/FIS/UI0068/2011 and PTDC/FIS-ATO/1832/2012 through FCT-MEC. The European Commission is acknowledged for a Marie Curie Intra-European Reintegration Grant (MERG-CT-2007-207292). Some of this work forms part of the EU/ESF COST Action Nano-IBCT-MP1002. R.P. acknowledges his visiting research fellowship at the OU.

[1]C. T. Middleton, K. de La Harpe, C. Su, Y. K. Law, C. E. Crespo-Hernandez, and B. Kohler, Annu. Rev. Phys. Chem. **60**, 217 (2009).
[2]M. K. Shukla and J. Leszczynski, J. Phys. Chem. A **106**, 8642 (2002).
[3]C. Canuel, M. Mons, F. Piuzzi, B. Tardivel, I. Dimicoli, and M. Elhanine, J. Chem. Phys. **122**, 074316 (2005).
[4]S. Ullrich, T. Schultz, M. Z. Zgierski, and A. Stolow, Phys. Chem. Chem. Phys. **6**, 2796 (2004).
[5]S. Matsika, C. Y. Zhou, M. Kotur, and T. C. Weinacht, Faraday Discuss. **153**, 247 (2011).
[6]D. Nachtigallova, A. J. A. Aquino, J. J. Szymczak, M. Barbatti, P. Hobza, and H. Lischka, J. Phys. Chem. A **115**, 5247 (2011).
[7]A. Gedanken, M. B. Robin, and N. A. Kuebler, J. Phys. Chem. **86**, 4096 (1982).
[8]T. Gustavsson, A. Banyasz, E. Lazzarotto, D. Markovitsi, G. Scalmani, M. J. Frisch, V. Barone, and R. Improta, J. Am. Chem. Soc. **128**, 607 (2006).
[9]M. Etinski and C. M. Marian, Phys. Chem. Chem. Phys. **12**, 4915 (2010).
[10]Y. G. He, C. Y. Wu, and W. Kong, J. Phys. Chem. A **108**, 943 (2004).
[11]P. Colarusso, K. Zhang, B. Guo, and P. F. Bernath, Chem. Phys. Lett. **269**, 39 (1997).
[12]M. Schneider, C. Schon, I. Fischer, L. Rubio-Lago, and T. Kitsopoulos, Phys. Chem. Chem. Phys. **9**, 6021 (2007).
[13]R. Tembreull and D. M. Lubman, Anal. Chem. **59**, 1082 (1987).
[14]C. H. Lin, J. Matsumoto, S. Ohtake, and T. Imasaka, Talanta **43**, 1925 (1996).
[15]B. B. Brady, L. A. Peteanu, and D. H. Levy, Chem. Phys. Lett. **147**, 538 (1988).
[16]S. H. Nam, H. S. Park, J. K. Song, and S. M. Park, J. Phys. Chem. A **111**, 3480 (2007).
[17]H. Kang, K. T. Lee, B. Jung, Y. J. Ko, and S. K. Kim, J. Am. Chem. Soc. **124**, 12958 (2002).
[18]Y. G. He, C. Y. Wu, and W. Kong, J. Phys. Chem. A **107**, 5145 (2003).
[19]M. Etinski, T. Fleig, and C. M. Marian, J. Phys. Chem. A **113**, 11809 (2009).
[20]M. T. Nguyen, R. Zhang, P. C. Nam, and A. Ceulemans, J. Phys. Chem. A **108**, 6554 (2004).
[21]H. W. Jochims, M. Schwell, H. Baumgartel, and S. Leach, Chem. Phys. **314**, 263 (2005).
[22]C. Lecompte, G. Mainfray, C. Manus, and F. Sanchez, Phys. Rev. A **11**, 1009 (1975).
[23]M. Imhoff, Z. Deng, and M. Huels, Int. J. Mass Spectrom. **262**, 154 (2007).
[24]J. M. Rice, G. O. Dudek, and M. Barber, J. Am. Chem. Soc. **87**, 4569 (1965).
[25]S. Denifl, B. Sonnweber, G. Hanel, P. Scheier, and T. D. Märk, Int. J. Mass Spectrom. **238**, 47 (2004).
[26]S. Feil, K. Gluch, S. Matt-Leubner, P. Scheier, J. Limtrakul, M. Probst, H. Deutsch, K. Becker, A. Stamatovic, and T. D. Märk, J. Phys. B **37**, 3013 (2004).
[27]See http://webbook.nist.gov for NIST Chemistry WebBook; accessed 2013.
[28]B. Coupier, B. Farizon, M. Farizon, M. J. Gaillard, F. Gobet, N. V. de Castro Faria, G. Jalbert, S. Ouaskit, M. Carré, B. Gstir, G. Hanel, S. Denifl, L. Feketeova, P. Scheier, and T. D. Märk, Eur. Phys. J. D **20**, 459 (2002).
[29]J. Tabet, S. Eden, S. Feil, H. Abdoul-Carime, B. Farizon, M. Farizon, S. Ouaskit, and T. D. Mark, Phys. Rev. A **81**, 012711 (2010).
[30]A. Le Padellec, P. Moretto-Capelle, M. Richard-Viard, J. P. Champeaux, and P. Cafarelli, J. Phys.: Conf. Ser. **101**, 012007 (2008).
[31]T. Schlathölter, F. Alvarado, and R. Hoekstra, Nucl. Instrum. Methods Phys. Res. B **233**, 62 (2005).
[32]T. Schlathölter, F. Alvarado, S. Bari, A. Lecointre, R. Hoekstra, V. Bernigaud, B. Manil, J. Rangama, and B. Huber, ChemPhysChem **7**, 2339 (2006).
[33]J. de Vries, R. Hoekstra, R. Morgenstern, and T. Schlathölter, Phys. Scr. **T110**, 336 (2004).
[34]J. de Vries, R. Hoekstra, R. Morgenstern, and T. Schlathölter, J. Phys. B **35**, 4373 (2002).
[35]J. de Vries, R. Hoekstra, R. Morgenstern, and T. Schlathölter, Phys. Rev. Lett. **91**, 053401 (2003).
[36]C. Zhou, S. Matsika, M. Kotur, and T. C. Weinacht, J. Phys. Chem. A **116**, 9217 (2012).
[37]L. S. Arani, P. Mignon, H. Abdoul-Carime, B. Farizon, M. Farizon, and H. Chermette, Phys. Chem. Chem. Phys. **14**, 9855 (2012).
[38]I. Hünig, C. Plützer, K. A. Seefeld, D. Löwenich, M. Nispel, and K. Kleinermanns, ChemPhysChem **5**, 1427 (2004).
[39]W. Li, S. A. Lahankar, C. Huang, P. S. Shternin, O. S. Vasyutinskii, and A. G. Suits, Phys. Chem. Chem. Phys. **8**, 2950 (2006).
[40]A. Dogariu and R. B. Miles, Appl. Opt. **50**, A68 (2011).
[41]S. R. Gadre, K. Babu, and A. P. Rendell, J. Phys. Chem. A **104**, 8976 (2000).
[42]T. van Mourik, S. L. Price, and D. C. Clary, J. Phys. Chem. A **103**, 1611 (1999).
[43]T. van Mourik, D. M. Benoit, S. L. Price, and D. C. Clary, Phys. Chem. Chem. Phys. **2**, 1281 (2000).
[44]V. B. Delchev, I. G. Shterev, and H. Mikosch, Monatsh. Chem. **139**, 349 (2008).
[45]V. I. Danilov, T. van Mourik, and V. I. Poltev, Chem. Phys. Lett. **429**, 255 (2006).

[46]T. van Mourik, V. I. Danilov, V. V. Dailidonis, N. Kurita, H. Wakabayashi, and T. Tsukamoto, Theor. Chem. Acc. **125**, 233 (2010).
[47]N. J. Kim, H. Kang, G. Jeong, Y. S. Kim, K. T. Lee, and S. K. Kim, Proc. Natl. Acad. Sci. U.S.A. **98**, 4841 (2001).
[48]S. K. Kim, W. Lee, and D. R. Herschbach, J. Phys. Chem. **100**, 7933 (1996).
[49]See http://winter.group.shef.ac.uk/chemputer/ for M. Winter, University of Sheffield; accessed 2013.
[50]R. Mota, R. Parafita, A. Giuliani, M.-J. Hubin-Franskin, J. M. C. Lourenço, G. Garcia, S. V. Hoffmann, N. J. Mason, P. A. Ribeiro, M. Raposo, and P. Limão-Vieira, Chem. Phys. Lett. **416**, 152 (2005).
[51]A. A. Zadorozhnaya and A. I. Krylov, J. Chem. Theory Comput. **6**, 705 (2010).
[52]A. M. Rasmussen, M. C. Lind, S. Kim, and H. F. Schaefer III, J. Chem. Theory Comput. **6**, 930 (2010).